onto M9 plates containing amp, Trp, and Leu, and lacking uracil. The yeast *URA3* gene complements the Ura$^-$ phenotype of *E. coli pyrF* mutants [M. Rose, P. Grisafi, D. Botstein, *Gene* **29**, 113 (1984)]. This *E. coli* screen eliminated mutant plasmids that did not express a functional Ura3 moiety of Ub-Arg-DHFR-ha-Ura3 at 37°C. However, those (potentially relevant) plasmids that expressed a mutant DHFR moiety were expected to pass this test. [*E. coli* lacks the ubiquitin system (*6*). The N-terminal ubiquitin moiety of Ub-Arg-DHFR-ha-Ura3 was therefore retained in *E. coli*, precluding the formation of an N-degron.]

10. Plasmids that passed the *E. coli* screen (*9*) were introduced into *S. cerevisiae* YPH500 (*his3 ura3*) (*18*), with transformants selected at 23°C on SD(-Ura) plates containing 0.1 mM $CuSO_4$. The colonies were replica-plated onto SD plates (*20*) lacking His (to select for plasmid retention) and containing 5-fluoroorotic acid (FOA) and uracil [J. D. Boeke, F. Lacroute, G. R. Fink, *Mol. Gen. Genet.* **197**, 345 (1984)]. The FOA plates were incubated at 37°C to select against cells (carrying pPW17R plasmids) that could yield a functional Ura3 at 37°C. (FOA kills Ura3$^+$ cells.) After several rounds of the FOA-mediated selection against cells that were Ura$^+$ at 37°C, we verified the *ts* Ura$^+$ phenotype of surviving cell clones by replica-plating them onto SD(-Ura, -His) plates at 37°C. Plasmids from cells that passed these screens were introduced into the YPH500-derived strain JD15 [*ubr1-Δ1::LEU2 ura3*, produced identically to *ubr1Δ* strains in (*11, 12*)], with transformants selected on SD(-Ura) plates at 37°C. This step narrowed the selection to plasmids whose ability to confer the *ts* Ura$^+$ phenotype required the presence of the N-end rule pathway (*6, 11, 12*). In both of the plasmids thus obtained, the *ts* lesion was found to be a single missense mutation in the region encoding DHFR (see text). The mutation was identified by first determining, in restriction fragment-swapping tests, that the relevant alteration resided within the DHFR moiety of Ub-Arg-DHFR-ha-Ura3, and then by sequencing the DHFR-coding regions in the initial (pPW17R) and mutant plasmids using the chain termination method (*20*). The final construct, termed pPW43R, was produced from the unmutagenized pPW17R by replacement of its Eco RI fragment encoding Ub-Arg-DHFR-ha-Ura3 with the otherwise identical fragment from one of the above plasmids encoding Ub-Arg-DHFR^{ts}-ha-Ura3.
11. B. Bartel, I. Wünning, A. Varshavsky, *EMBO J.* **9**, 3179 (1990).
12. K. Madura, R. J. Dohmen, A. Varshavsky, *J. Biol. Chem.* **268**, 12046 (1993).
13. C. Oefner, A. D'Arcy, F. K. Winkler, *Eur. J. Biochem.* **174**, 377 (1988); K. W. Volz *et al.*, *J. Biol. Chem.* **257**, 2528 (1982).
14. S. I. Reed, *Annu. Rev. Cell Biol.* **8**, 529 (1992); A. W. Murray, *Nature* **359**, 599 (1992); A. B. Futcher, *Semin. Cell. Biol.* **2**, 205 (1991); K. Nasmyth, L. Dirick, U. Surana, A. Amon, F. Cvrčkova, *Cold Spring Harbor Symp. Quant. Biol.* **56**, 9 (1991); P. Nurse, *Nature* **344**, 503 (1990).
15. The plasmid pPW66R was constructed in the background of the *URA3*-based integration vector pRS306 (*18*). Briefly, a DNA fragment encoding Ub-Arg-DHFR^{ts}-ha (*10*) was ligated to a fragment [produced using polymerase chain reaction and *S. cerevisiae* genomic DNA (*20*)] that encompassed the first 284 nucleotides of the *CDC28* open reading frame (ORF) (*14*). The resulting fragment, encoding Ub-Arg-DHFR^{ts}-ha-Cdc28$_{1-95}$, was positioned downstream from the P_{CUP1} promoter in pRS306, yielding pPW66R. This plasmid was linearized at the Msc I site (nucleotide 92 in the *CDC28* ORF) and transformed into *S. cerevisiae* YPH500 (*18*). In the resulting Ura$^+$ integrants, homologous recombinations [R. Rothstein, *Methods Enzymol.* **194**, 281 (1991)] between the *CDC28* region in pPW66R and *CDC28* in chromosome II (*14*) resulted in the integration of pPW66R and formation of an ORF encoding Ub-Arg-DHFR^{ts}-ha-Cdc28 (which contained the full-length CDC28$_{1-299}$ moiety), in addition to a nearby sequence encoding Cdc28$_{1-95}$. This truncated allele of *CDC28* was neither functional nor dominant negative.
16. E. C. Park, D. Finley, J. W. Szostak, *Proc. Natl. Acad. Sci. U.S.A.* **89**, 1249 (1992); B. P. Cormack and K. Struhl, *Cell* **69**, 685 (1992).
17. J. Johnston, E. Johnson, J. Dohmen, A. Varshavsky, unpublished results.
18. R. S. Sikorski and P. Hieter, *Genetics* **122**, 19 (1989).
19. E. S. Johnson, B. Bartel, W. Seufert, A. Varshavsky, *EMBO J.* **11**, 497 (1992); R. J. Dohmen, K. Madura, B. Bartel, A. Varshavsky, *Proc. Natl. Acad. Sci. U.S.A.* **88**, 7351 (1991).
20. F. M. Ausubel *et al.*, *Current Protocols in Molecular Biology* (Wiley-Interscience, New York, 1989).

21. We thank N. Kleckner (Harvard University) for the gift of plasmids and members of this laboratory, especially E. Johnson, K. Madura, F. Lévy, C. Byrd, and T. Clandinin, for plasmids and strains and for advice and comments on the manuscript. Supported by grants to A.V. from the National Institutes of Health. R.J.D. was supported by a postdoctoral fellowship from the European Molecular Biology Organization.

27 September 1993; accepted 21 January 1994

Open "Back Door" in a Molecular Dynamics Simulation of Acetylcholinesterase

M. K. Gilson,* T. P. Straatsma, J. A. McCammon, D. R. Ripoll, C. H. Faerman, P. H. Axelsen, I. Silman, J. L. Sussman

The enzyme acetylcholinesterase generates a strong electrostatic field that can attract the cationic substrate acetylcholine to the active site. However, the long and narrow active site gorge seems inconsistent with the enzyme's high catalytic rate. A molecular dynamics simulation of acetylcholinesterase in water reveals the transient opening of a short channel, large enough to pass a water molecule, through a thin wall of the active site near tryptophan-84. This simulation suggests that substrate, products, or solvent could move through this "back door," in addition to the entrance revealed by the crystallographic structure. Electrostatic calculations show a strong field at the back door, oriented to attract the substrate and the reaction product choline and to repel the other reaction product, acetate. Analysis of the open back door conformation suggests a mutation that could seal the back door and thus test the hypothesis that thermal motion of this enzyme may open multiple routes of access to its active site.

The enzyme acetylcholinesterase (AChE) terminates signaling at cholinergic synapses by rapid hydrolysis of the neurotransmitter acetylcholine (ACh). The crystal structure of AChE (*1*) raises questions regarding substrate entry and product release. First, the active site gorge is very deep and appears too narrow to admit ACh (*1, 2*). However, the demonstration that quaternary amines enter the active site of crystallized AChE (*3*) proves that the protein is sufficiently flexible to admit substrate by some route. Second, the inward electrostatic field at the gorge, which is likely to accelerate penetration of the positively charged substrate (*4, 5*), would seem to impede the exit of the product choline from the mouth of the active site. A thin wall near the base of the active site, at residues Met^{83} and Trp^{84}, could offer an alternative route for the escape of products (*4*). This back door might also provide a vent for water molecules during the passage of substrate, products, or both through the narrow gorge. We have studied these issues by performing a molecular dynamics (MD) simulation of AChE and analyzing the resulting time series of protein conformations with regard to active site accessibility.

Unobserved atoms were added to the *Torpedo californica* AChE dimer (*1*), as described in (*5*), using the program Quanta (Molecular Simulations, Waltham, Massachusetts). Protonation states at neutral pH were assigned on the basis of atomic solvent accessibilities, of salt-bridging and hydrogen-bonding opportunities, and of the putative catalytic mechanism, which requires the active site His^{440} to be neutral (*6*). The model enzyme was immersed in water, and the classical laws of motion solved numerically with weak coupling to a heat bath at 300 K to generate 119 ps of analyzable conformations (*7*).

We searched for conformations in which the active site had any aperture large enough to pass a water molecule, generating for each conformation a Lee and Richards (*8*) solvent-accessible dot surface with a 1.4 Å probe. The molecular

M. K. Gilson, T. P. Straatsma, J. A. McCammon, Department of Chemistry, University of Houston, Houston, TX 77204–5641, USA.
D. R. Ripoll, Cornell Theory Center, Cornell University, Ithaca, NY 14853–3801, USA.
C. H. Faerman, Section of Biochemistry, Molecular and Cell Biology, Cornell University, Ithaca, NY 14853, USA.
P. H. Axelsen, Department of Pharmacology, University of Pennsylvania School of Medicine, Philadelphia, PA 19104–6084, USA.
I. Silman, Department of Neurobiology, The Weizmann Institute of Science, Rehovot 76100, Israel.
J. L. Sussman, Department of Structural Biology, The Weizmann Institute of Science, Rehovot 76100, Israel.
*To whom correspondence should be addressed.

surface was separated into the outer surface and some number of cavity surfaces, based on distances between surface points (9). Of these surface subsets, the active site surface was defined as that contacted by Glu^{199} OE2, because this atom was consistently at the surface of the active site interior. Conformations with an open active site were those in which the numbers of connected points in both the active site and outer surfaces were identical.

Conformations with an open back door were sought as follows. For each conformation having an open active site, the active site entry was blocked by the deletion of all surface points within 8 Å of a point located approximately in the middle of residues Glu^{73}, Asn^{280}, Asp^{285}, and Leu^{333} that defines the entrance to the gorge. If the active site surface was still continuous with the outer surface of the enzyme, an alternative aperture existed.

This surface analysis detected a transient opening, occurring in the first 20 ps of production MD and persisting for 0.3 ps. A channel (Fig. 1) formed in the thin active site wall at Trp^{84}, the side chain of which probably contributes to binding of the quaternary ammonium of ACh (*1, 3, 10*). The channel began near Trp^{84} CH2 and CZ2, Gly^{441}, and the ring of Tyr^{442} and curved around the edge of Trp^{84} to emerge at a surface dimple near Glu^{445}. Its path led directly through a solvent-sized cavity that is observed in the crystal structure and which lies near Val^{129}. The displacement of the Trp^{84} indole, relative to its location in the crystal structure, resembles that of a camera shutter because it is completely in-plane.

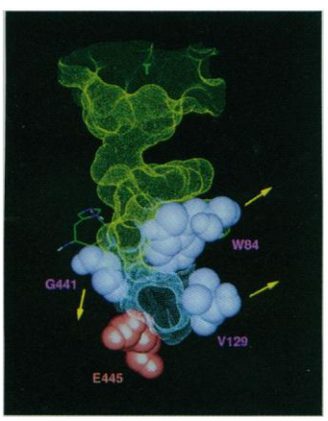

Fig. 1. Active site gorge with open back door. Green dots, solvent-accessible surface of active-site gorge (T, top of gorge); white dots, channel to back door. Space-filling atoms are shown for Trp^{84} (W84), Val^{129} (V129), Gly^{441} (G441), and Glu^{445} (E445). Vectors indicate directions of displacement of three of these residues relative to their positions in the crystal structure. Stick diagrams indicate catalytic residues His^{440} and Ser^{200}.

The channel can be opened by shifting only residues Trp^{84}, Val^{129}, and Gly^{441} from their crystal coordinates to their positions in the open conformation. The average atomic displacement for these residues, relative to the crystal conformation, is only 1.3 Å. The Trp^{84} residue is somewhat more mobile than average: The average root-mean-square (rms) fluctuation of its nonhydrogen atoms is 1.2 Å (main chain 0.8 Å, side chain 1.4 Å), compared with 0.72 Å for all nonhydrogen atoms within 25 Å of the dynamical center. The Val^{129} and Gly^{441} residues have unremarkable rms fluctuations of 0.70 Å.

Several points are significant to this opening mode. First, the time required for AChE to hydrolyze one substrate molecule is about 0.1 ms (*11*). Thus, although the observed opening event is brief, that it occurs at all in a 119-ps simulation suggests that the back door can play a functional role on the longer time scale of catalysis. Second, the small size of the atomic displacements required to open the back door means that the open conformation should be easy to achieve; experiments have demonstrated that protein structures fluctuate substantially (*12*). Third, the presence in the crystal structure of a solvent-sized cavity in the thin wall of the active site where the channel forms suggests that the x-ray data may reflect similar opening events in a time-averaged fashion. Finally, no opening events were observed in other portions of the active site wall, although every stored conformation was analyzed. Thus, Trp^{84} defines the only permeable part of the active site wall in this simulation.

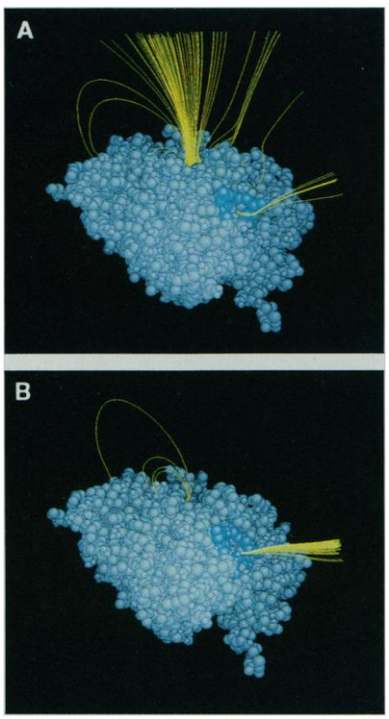

Fig. 2. Electric field lines for AChE with (**A**) open and (**B**) closed back door. The field lines (yellow) are traced from the region of negative potential near Glu^{199} OE2 deep in the active site. Blue atoms highlight the opening to the active site gorge. The back door is clearly marked by the vertical bundle of field lines in (A). Field lines were computed and displayed with GRASP (*16*). The orientation is changed relative to Fig. 1.

Because AChE appears to generate a functionally important electrostatic field (*4, 5*), we examined the effect of the open back door on this field (*13*). When the back door is open, field lines initiated at the active site Glu^{199}, near Trp^{84}, exit preferentially through this aperture (Fig. 2A). However, for the crystal structure most of these field lines emerge from the mouth of the active site gorge (Fig. 2B). When the electrostatic potential was evaluated at each point on a Lee and Richards–type surface (*8*), the surface point with the lowest electrostatic potential lay at the bottom of the active site, near Ile^{444}. Therefore, ACh and choline are attracted to the base of the gorge, either through the front or the back door. This observation militates against the idea that the same field that guides ACh into and down the gorge urges choline out the back door. However, the field accelerates the departure of the other product, acetate ion. Also, a more widely opened back door might significantly weaken the active site fields by increasing exposure of the active site to the high dielectric solvent. This effect would facilitate the release of choline.

One way to test whether a functionally important back door does exist would be a kinetic study of a mutant enzyme whose back door is sealed. Of the three residues whose movement opens the channel, Trp^{84}, Val^{129}, and Gly^{441}, it appears that only Val^{129} could be modified without the disruption of enzyme function by undesired mechanisms. Steric analysis of the crystal structure suggests that a Lys or Arg would fit well at position 129, with the positive group between Met^{83}, Asp^{128}, Glu^{445}, and Leu^{456} (Fig. 1). In this position, the side chain would fill the surface dimple where the back door channel emerges. The positive group of the mutant side chain would be far (~11 Å) from the interior of the active site. To our knowledge, no special role has been suggested for Val^{129}, and because it lies at the protein surface, it appears to be structurally unimportant. However, aligned cholinesterase amino acid sequences show little variation at this position: Eight have Val and two have Ile (*14*). Isoleucine seems unlikely to block the back door because it possesses only one more methylene than Val. If the mutation of Val^{129} does slow the enzyme, it will be necessary to confirm the absence of structural distortion through crystallographic studies.

Experiments have shown that thermal fluctuations make proteins somewhat porous, especially to small, nonpolar molecules (*15*). Our analysis supports the concept that the active site of AChE has a particularly porous wall at Trp^{84}, which may be of functional importance. Kinetic energy gained by the catalytic residue His^{440} during hydrolysis may pass by way of the peptide linkage to Gly^{441}, one of the channel residues. This energy might increase the probability of opening, causing an organized sequence of catalysis and channel opening.

REFERENCES AND NOTES

1. J. L. Sussman *et al.*, *Science* **253**, 872 (1991).
2. P. H. Axelsen, M. Harel, I. Silman, J. L. Sussman, *Protein Sci.*, in press.
3. M. Harel *et al.*, *Proc. Natl. Acad. Sci. U.S.A.* **90**, 9031 (1993).
4. D. R. Ripoll, C. H. Faerman, P. H. Axelsen, I. Silman, J. L. Sussman, *ibid.*, p. 5128.
5. R. C. Tan, T. N. Truong, J. A. McCammon, J. L. Sussman, *Biochemistry* **32**, 401 (1993).
6. All Arg, Lys, Asp, Glu, NH_2-terminal, and COOH-terminal groups were assigned "ionized" (except Glu^{443}). The Glu^{443} residue was assigned "neutral" (OE2 protonated) because it is fully desolvated and appears to form only two to three hydrogen bonds. All Tyr and Cys side chains were set neutral. Histidine protonation sites were His^{3}, ND1; His^{26}, ND1; His^{159}, NE2; His^{181}, ND1, NE2; His^{209}, NE2; His^{264}, ND1; His^{362}, ND1; His^{398}, ND1; His^{406}, ND1, NE2; His^{425}, ND1, NE2; His^{440}, ND1; His^{471}, ND1, NE2; His^{486}, NE2; and His^{513}, ND1, NE2. The net charge per monomer was −5. Both monomers were assigned identical protonation states. Polar hydrogens were added with the ARGOS package (*17*).
7. With only crystallographic solvent included, the energy was minimized with respect to hydrogen positions for 200 steepest descent steps. The energy was then minimized for 200 steepest descent steps with respect to the coordinates of residues 535 to 537 and 1072 to 1074 to form the COOH-terminal disulfide bond. A pre-equilibrated box of waters [SPC/E model (*18*)] was overlayed repeatedly on the system to fill in a 40 Å sphere centered on atom NE2 of the catalytic His^{440}. The 142 crystallographic waters were retained. Waters closer than 2.5 Å to any crystallographic heavy atom were rejected. Atoms more than 35 Å from His^{440} NE2 were fixed in space for all subsequent calculations to create a constant-volume dynamical system containing 5252 protein atoms and 3117 water molecules. Energy was minimized with respect to water coordinates for 200 steepest descent steps. Then MD on water only was performed for 20 ps, with velocity reassignment at 300 K every 0.2 ps and velocity rescaling (*19*) with time constant 0.2 ps. Energy was then minimized with respect to protein coordinates for 200 steepest descent steps. MD on the protein only was performed for three segments of 5 ps each, with velocity reassignment every 0.2 ps and rescaling with time constant 0.1 ps, at 100 K, 200 K, and 300 K, respectively. Before production calculations were made, MD was used to equilibrate the entire system for 20 ps at 300 K, with separate solute and solvent velocity rescaling with time constant 0.2 ps. During the first 20 ps of production, coordinates were stored every 20 steps. Subsequently, coordinates were stored every five steps. All interactions in a short-range (10 Å) pair list [illegible] while all interactions in a [illegible] were updated every five steps. Separate solvent-solvent, solvent-solute, and solute-solute pair lists were updated every 10, 15, and 20 steps, respectively. Pair lists were based on charge groups. SHAKE (*20, 21*) was used to constrain bond lengths, permitting the use of a 2-fs time step. All calculations were made with the ARGOS program package (*17*), with GROMOS atomic parameters (*22*). System temperatures approximated 301 K, with solute temperatures of about 298 K and solvent temperatures of about 302 K. Total system potential energy averaged -200×10^3 kJ mol^{-1}, with a drift of −8.0 kJ mol^{-1} ps^{-1} during the final 100 ps. During the final 100 ps, the rms atomic position deviation from crystal coordinates of nonhydrogen atoms in the innermost 25 Å of the simulation sphere averaged 1.7 Å, with a residual upward slope of 0.001 Å ps^{-1}.
8. B. Lee and F. M. Richards, *J. Mol. Biol.* **55**, 379 (1971).
9. Surface generation started with 100 surface points per atom, representing possible locations of the center of a solvent probe sphere. For simplicity, hydrogen atoms were excluded, and all heavy atoms were assigned a radius of 1.8 Å. Two surface points were assigned to the same surface subset if they were closer than the greatest distance between any point and its nearest neighbor on the initial 100-point surface sphere of each atom.
10. C. Weise *et al.*, *EMBO J.* **9**, 3885 (1990).
11. M. Vigny, S. Bon, J. Massoulié, F. Leterrier, *Eur. J. Biochem.* **85**, 317 (1978).
12. S. Englander and N. Kallenbach, *Q. Rev. Biophys.* **16**, 521 (1984).
13. We used the finite-difference Poisson-Boltzmann method (*23*), implemented in the program UHBD (*24*) to compute electrostatic fields in and around AChE. Finite-difference Poisson-Boltzmann calculations were made with protein and solvent dielectric constants of 2 and 80, respectively, physiologic ionic strength (150 mM), and a 2.0 Å Stern layer. The dielectric boundary was defined as the Richards (*25*) probe-accessible surface. The only source charges were the formally charged groups of the molecular dynamics calculation. We used a 65 by 65 by 65 point grid with 1.5 Å spacing.
14. M. Cygler *et al.*, *Protein Sci.* **2**, 366 (1993).
15. A. P. Demchenko, *Essays Biochem.* **22**, 120 (1986).
16. GRASP, vers. 1.04; A. Nicholls and B. Honig, Columbia University, New York.
17. T. P. Straatsma and J. A. McCammon, *J. Comput. Chem.* **11**, 943 (1990).
18. H. J. C. Berendsen, J. R. Grigera, T. P. Straatsma, *J. Phys. Chem.* **91**, 6269 (1987).
19. H. J. C. Berendsen, J. P. M. Postma, W. F. van Gunsteren, A. DiNola, J. R. Haak, *J. Chem. Phys.* **81**, 3684 (1984).
20. W. F. van Gunsteren and H. J. C. Berendsen, *Mol. Phys.* **34**, 1311 (1977).
21. J.-P. Ryckaert, G. Ciccotti, H. J. C. Berendsen, *J. Comput. Phys.* **23**, 327 (1977).
22. W. F. van Gunsteren and H. J. C. Berendsen, *Groningen Molecular Simulation* (GROMOS) *Library Manual* (Biomos, Groningen, Netherlands, 1987).
23. J. Warwicker and H. C. Watson, *J. Mol. Biol.* **157**, 671 (1982); I. Klapper, R. Hagstrom, R. Fine, K. Sharp, B. Honig, *Proteins Struct. Func. Gen.* **1**, 47 (1986); M. K. Gilson, K. A. Sharp, B. H. Honig, *J. Comput. Chem.* **9**, 327 (1988).
24. M. E. Davis, J. D. Madura, B. A. Luty, J. A. McCammon, *Comput. Phys. Commun.* **62**, 187 (1991).
25. F. M. Richards, *Annu. Rev. Biophys. Bioeng.* **6**, 151 (1977).
26. Atomic coordinates for the open back door conformation are available by anonymous Internet file transfer program (ftp) to mrbun.chem.uh.edu. We thank B. Honig and A. Nicholls for making available the graphics program GRASP and R. Gillilan and H. S. R. Gilson for helpful discussions. Supported by the Robert A. Welch Foundation, the National Institutes of Health, the National Science Foundation, the Grand Challenge Program of the National Science Foundation supercomputer centers, the Minerva Foundation, the Kimmelman Center, and U.S. Army Medical Research and Development Command Contract no. DAMD17-93-C-3070. M.K.G. is a Howard Hughes Physician Research Fellow and I.S. is Bernstein-Mason Professor of Neurochemistry. P.H.A. is supported by the Markey Charitable Trust.

10 August 1993; accepted 15 November 1993

Suppression of Ras-Induced Transformation of NIH 3T3 Cells by Activated $G\alpha_s$

Jianghao Chen and Ravi Iyengar*

Conversion of external signals into proliferative responses may be mediated by interactions between signaling pathways that control cell proliferation. Interactions between $G\alpha_s$, the α subunit of the heterotrimeric guanine nucleotide binding protein that stimulates adenylyl cyclase, and Ras, an important element in growth factor signaling, were studied. Expression of activated $G\alpha_s$ in NIH 3T3 cells increased intracellular concentrations of adenosine 3′,5′-monophosphate (cAMP) and inhibited H-Ras–stimulated DNA synthesis and mitogen-activated protein kinase activity. Activated $G\alpha_s$ and 8-Br-cAMP suppressed H-Ras–induced transformation of NIH 3T3 cells. Apparently, $G\alpha_s$ inhibits proliferative signals from Ras by stimulating cAMP production and activating protein kinase A.

Many heterotrimeric guanine nucleotide binding proteins (G proteins) participate in mitogenic signaling (*1*). Of these, the G_s and its signaling pathway are probably the most enigmatic. In a few systems, receptor activation of the cAMP pathway is mitogenic (*2*), but in most systems raising the intracellular concentration of cAMP has no effect on cell proliferation. An activated mutant form of $G\alpha_s$ has been identified in pituitary tumors and postulated to be an oncogene (*3*), but has not been shown to transform cells in vitro. Thus $G\alpha_s$ might not produce a strong proliferative signal by itself, but it might have effects in conjunc-

J. Chen, Department of Biochemistry, Mount Sinai School of Medicine, City University of New York, NY 10029, USA.
R. Iyengar, Department of Pharmacology, Mount Sinai School of Medicine, City University of New York, One Gustave L. Levy Place, New York, NY 10029, USA.
*To whom correspondence should be addressed.